in vivo *28*: 411-424 (2014)

Cryopreservation of Viable Human Lung Tissue for Versatile Post-thaw Analyses and Culture

JOHN E. BAATZ[1], DANFORTH A. NEWTON[1], ELLEN C. RIEMER[2], CHADRICK E. DENLINGER[3], E. ELLEN JONES[4], RICHARD R. DRAKE[4] and DEMETRI D. SPYROPOULOS[2]

Departments of [1]Pediatrics, [2]Pathology and Laboratory Medicine, [3]Surgery, [4]Pharmacology, Medical University of South Carolina, Charleston, SC, U.S.A.

Abstract. *Clinical trials are currently used to test therapeutic efficacies for lung cancer, infections and diseases. Animal models are also used as surrogates for human disease. Both approaches are expensive and time-consuming. The utility of human biospecimens as models is limited by specialized tissue processing methods that preserve subclasses of analytes (e.g. RNA, protein, morphology) at the expense of others. We present a rapid and reproducible method for the cryopreservation of viable lung tissue from patients undergoing lobectomy or transplant. This method involves the pseudo-diaphragmatic expansion of pieces of fresh lung tissue with cryoprotectant formulation (pseudo-diaphragmatic expansion-cryoprotectant perfusion or PDX-CP) followed by controlled-rate freezing in cryovials. Expansion-perfusion rates, volumes and cryoprotectant formulation were optimized to maintain tissue architecture, decrease crystal formation and increase long-term cell viability. Rates of expansion of 4 cc/min or less and volumes ranging from 0.8-1.2 × tissue volume were well-tolerated by lung tissue obtained from patients with chronic obstructive pulmonary disease or idiopathic pulmonary fibrosis, showing minimal differences compared to standard histopathology. Morphology was greatly improved by the PDX-CP procedure compared to simple fixation. Fresh versus post-thawed lung tissue showed minimal differences in histology, RNA integrity numbers and post-translational modified protein integrity (2-dimensional differential gel electrophoresis). It was possible to derive numerous cell types, including alveolar epithelial cells, fibroblasts and stem cells, from the tissue for at least three months after cryopreservation. This new method should provide a uniform, cost-effective approach to the banking of biospecimens, with versatility to be amenable to any post-acquisition process applicable to fresh tissue samples.*

Correspondence to: John E. Baatz, Ph.D., Department of Pediatrics, Medical University of South Carolina, C.P. Darby Children's Research Institute, MSC 513, 173 Ashley Avenue, Charleston, SC 29425, U.S.A. Tel: +1 8437921049, e-mail: baatzje@musc.edu

Key Words: Cryopreservation, lung, biorepository, biobank.

Lung injury and disease in humans has profound socioeconomic impact, and lung cancer remains by far the most common cancer in the U.S. Smoking-related lung cancer, ischemic heart disease, and chronic airways obstruction deaths in the US cost $96 billion annually (1). However, advances in the diagnosis and treatment of such conditions are severely hampered by expensive, time-consuming and inadequate clinical sample acquisition and animal model systems. The 5-year survival rate for patients with lung cancer (16%) has not improved appreciably in the past 20 years (6, 10). A hallmark of these insufficiencies is the large strata of patients with diagnoses that are resistant to conventional treatments, indicative of patient sub-populations with alternate underlying mechanisms of disease or differing responses to treatments. Effective biospecimen collection and analysis hold the greatest promise for addressing these personalized medicine issues. Very large amounts of time, money and space are dedicated to biospecimen collection processing and storage (11, 12, 20); nevertheless, the biospecimens collected using current protocols fall short of their full potential utility for human disease research due to limitations with each of these various protocols (11, 12).

After acquisition, specimens are portioned and each portion handled and processed differently in order to stabilize or preserve different biomolecules. Thus, each specialized method preserves one class of biomolecules at the expense of others. For example, significant changes in gene and protein expression profiles have been detected after less than 12 min of cold ischemia time for colonic biospecimens (17) and most human biospecimens are not processed within this timeframe (5). Preservation of one class of biomolecular analyte leads to the loss of another, and methods for preservation of all classes of analytes are not available and thus not employed for individual biospecimens (5, 13, 15). An additional

problem, in particular with lung specimens, is that the architecture changes dramatically when the sample is not inflation-fixed, but then again, this sacrifices many aspects of biomolecular analyte analysis.

The development of simple methods for the preservation of 'fresh quality' lung tissue would provide a unified approach to lung tissue banking. Upon thawing, this viable lung tissue would then be amenable to all downstream analytical platforms applied to fresh tissue (*e.g.* DNA, RNA, protein, lipids, small molecules, cells, and histology). Multiple post-acquisition, pre-banking protocols currently utilized to capture subsets of molecules will no longer be necessary prior to banking. These numerous protocols need to be replaced because they preserve only a subset of molecules at the expense of others and cannot presuppose potentially novel user needs that fresh tissue can facilitate. To illustrate, we have compared the applicability of our new pseudo-diaphragmatic expansion-cryoprotectant perfusion (PDX-CP) method to previous protocols for specific analytical procedures (Table I).

Having access to lung biospecimens that maintain both cell viability and tissue architecture after thawing would greatly facilitate determination of the underlying mechanisms of lung injury, disease and cancer. Such cryopreserved lung samples would provide the material for rapidly assessing physiological impacts of exposures (biological/toxin) and therapeutic responsiveness. This resource would go beyond current cutting-edge preservation technologies (2, 7, 14, 21) and thus be amenable as new models for personalized lung disease, including those of chronic obstructive pulmonary disease (COPD), pulmonary arterial hypertension, idiopathic pulmonary fibrosis (IPF), bronchopulmonary dysplasia, emphysema and cancer. Several genome-wide assessment studies and clinical trials indicate that each of these disorders can be stratified into sub-groups for therapy: these new models could be used to more easily, and thus more cost-effectively stratify sub-groups of patients for specialized therapies. These tissue samples could serve as the sources for cell-, matrix-or scaffold-based 'bioengineered lungs' or simply as thawed lung tissue sections in *ex vivo* lung tissue-responsiveness studies. In both sets of studies, molecular signatures from later patient-specific needle biopsy or bronchiolar lavage could be used for predicting responsive *versus* refractory patient strata. For example, despite the use of surgery, chemotherapy and radiation in the treatment of lung cancer, the survival rate for patients has not improved appreciably (approximately 16% for five years) over the past 20 years (6, 10). This poor prognosis emphasizes an urgent need to improve the treatment for lung cancer and, in particular, to develop rapid and reliable methods to test the efficacy of antitumor drugs prior to clinical trial. High-throughput, 3-dimensional (3D) *in vitro* systems can be used to produce models to study lung disease therapies. However, establishing a link between these models and clinical responses in patients has not been obvious. Models to test the efficacy of antitumor drugs prior to clinical trial first have to be both rapid and reliable–not only capable of demonstrating tumor responses to dosing, but also usable for indicating drug interactions and accounting for inter-patient variation.

Herein we present an approach with the capacity for preserving 'fresh sample' quality lung biospecimens for storage, distribution and later use, all using the same procedure on all tissue available, obviating the need for multiple laboratory processing techniques, which is more time-consuming. This novel PDX-CP approach preserves lung biospecimens, such that after thawing, cell viability, tissue architecture and function are maintained. Our approach is an innovative technological leap forward for improving specifically lung tissue banking, and provides a fundamentally novel resource for lung research, especially in relation to the rapidly expanding cancer genomic and personalized medicine efforts. Unlike current protocols for preserving lung tissue for biorepositories, our approach offers the added ability to perform multiple molecular and cellular techniques in order to examine the underlying mechanisms of disease. Samples can be saved for later 'batching' of assays, for increased efficiency and cost-effectiveness in tissue analysis without sacrificing the fidelity of data obtained or biological response due to sample storage, freezing, *etc*.

Materials and Methods

Lung tissue source. Lung tissues targeted for cryopreservation were obtained under the Medical University of South Carolina Institutional Review Board for Human Research IRB approval from surgical lung transplant explants and lobectomies that were clinically necessitated for patients with defined lung pathologies, including cancer, emphysema, COPD, pulmonary arterial hypertension, or IPF. These samples were deemed 'excess tissue' not required for current or potential future diagnosis or patient care and subject to hospital disposition.

PDX-CP technique. A detailed initial description of our expansion perfusion cryopreservation technique and non-toxic cryoprotectant solution (sCP; comprised of 10% dimethyl sulfoxide (DMSO), 10% FCS and Dulbecco's Modified Eagle's Medium:Ham's F12 (DMEM-F12) media) has been published (9). Both the sCP formulation and technique have since been modified and optimized (now collectively called PDX-CP) for maintenance of cell viability and tissue architecture using a programmable syringe pump for controlled rate and volume expansion and cryoprotectant perfusion, rather than manual expansion or perfusion as previously published (9). Lung lobectomies from patients with COPD/lung cancer or lung explant tissue from lung transplant patients (typically diagnosed with IPF) were resected and placed in ice-cold 0.9% saline solution for processing within one hour of hypoxia (clamping of the major blood supply). Prior to processing, tissue strips were sectioned into small cubes (0.5-0.75 cm/edge; 0.13-0.42 cc volume), PDX-CP perfused with five volumes of non-toxic cryoprotectant solution, followed by controlled-rate freezing of samples (15-50 vials/patient; 1˚C/min to –80˚C). PDX perfusion was accomplished by placing cryoprotectant and tissue cubes in a Luer lock syringe equipped with a BD Connecta™ Plus stopcock (BD Biosciences, San Jose, CA, USA).

Table I. *Analytical utility of PDX-CP protocol versus current tissue preservation protocols used by biorepositories*.

		Preservation protocol					
Analyte	Analytical method	PDX-CP	RNAlater	HOPE	Flash Frozen	OCT blocks	PFA/FFPE
DNA	PCR	✓	✓	✓	✓	✓	✓
	Microarray	✓	✓	✓	✓	✓	
	ChIP/ChIP-on-chip	✓	✓	✓	✓		
	LCM	✓		✓		✓	
mRNA	RT-PCR	✓	✓	✓	✓	✓	✓
	qPCR	✓	✓	✓	✓	✓	
	Microarray	✓	✓	✓	✓		
	RNAseq	✓	✓	✓	✓		
	ISH/FISH	✓		✓	✓	✓	
Protein	Western/ELISA	✓	✓	✓	✓	✓	
	IHC	✓		✓	✓	✓	✓
	iTRAQ	✓					
	PTM *via* OrbiTrap	✓					
	SILAC	✓					
	MALDI Imaging/Mapping	✓					
	Antibody/Protein Array	✓	✓		✓		
	Qualitative 2D gel	✓	✓		✓		
	Quantitative 2D DIGE	✓					
	Tissue array	✓		✓			✓
Lipid	MALDI Imaging	✓					
	LC/MS	✓					
Other	H&E/morphometry	✓		✓			✓
	Primary cell culture	✓					
	Tissue culture	✓					

✓ = Appropriate protocol for method; ✓ = limited utility (depending upon storage temperature, thaw time and/or maintenance of protein PTM); PDX-CP, pseudo-diaphragmatic expansion cryoprotectant-perfusion; HOPE, hydroxyethyl piperazineethanesulfonic acid buffer-organic solvent protection effect; PFA, 4˚C paraformaldehyde; FFPE, formalin-fixed paraffin-embedded; PCR, polymerase chain reaction; ChIP, chromatin immunoprecipitation; LCM, laser capture microdissection; RT-PCR, reverse transcriptase PCR; qPCR, quantitative PCR; RNAseq, high-throughput RNA sequencing; ISH, *in situ* hybridization; FISH, fluorescence *in situ* hybridization; ELISA, enzyme-linked immunosorbent assay; IHC, immunohistochemistry; iTRAQ, isobaric tags for relative and absolute quantitation; PTM, post-translational modification; SILAC, stable isotope labeling by amino acids in cell culture; MALDI, matrix-assisted laser desorption mass spectrometry; DIGE, differential gel electrophoresis; LC/MS; liquid chromatography-coupled mass spectrometry; H&E, hematoxylin and eosin staining.

This device was placed into a programmable SPL syringe pump (#SPLG212; World Precision Instruments, Sarasota, FL, USA) to control rate and volume expansion, moving the syringe plunger slowly backwards to increase chamber volume (partial vacuum, tissue expansion/perfusion) and forwards to reduce chamber volume to atmospheric pressure (1 atm). Air was periodically removed from the device *via* stopcock and the process repeated six times. Directly-fixed (4% cold paraformaldehyde (PFA) overnight, dehydrated and embedded) or directly dissociated (15) pieces of fresh lung cubes were compared to PDX-CP pieces after thawing for a variety of analytes, as described below. For these studies, lung explants from IPF transplant recipients (n=4) and lung lobectomies from patients with COPD/lung cancer (total n=20) were used.

RNA integrity assessments. The Agilent 2100 Bioanalyzer (Agilent Technologies, Inc., Santa Clara, CA, USA) was used for measurements on fresh and thawed tissue or dissociated cells, since this equipment is arguably a standard in the field of biomolecular quality assessment. For RNA integrity numbers (RINs), RNA from dissociated cells was purified using the Absolutely RNA Nanoprep Kit (#400753; Agilent) and from tissue using the Absolutely RNA Miniprep Kit (#400800; Agilent) according to manufacturer and purified RNA was chip analyzed using the RNA 6000 Nano Chip kit [#5067-1511; Agilent; ref. (5)].

Protein integrity assessment. Protein measurements were carried out by placing tissue or cells into low-salt buffer (10 mM HEPES, 10 mM KCl, 0.1 mM EDTA, 1mM dithiothreitol (DTT), supplemented with protease and phosphatase inhibitors) containing 0.5% NP40 (Igepal CA-630; Sigma, St. Louis, MO, USA) and sonicated (tissue) or syringe-passaged (cells). Protein concentrations were determined using a MicroBCA Protein Assay Kit (Pierce Biotechnology, Rockford, IL, USA). Prior to chip analysis, protein preparations had a pH of 8.0-9.0. The High-Sensitivity Protein 250 Chip kit (#5067-1575; Agilent) was used according to the manufacturer to measure protein yield and integrity in the range of 10-250 kDa.

Cell isolation and culture. Cryopreserved lung tissues were thawed for 5 min in a water-bath at 37˚C, rinsed in balanced salt solution and, as with fresh tissue, enzymatically digested at 37˚C for 45 min in Luer-lock syringes (for perfusion) using a collagenase/dispase mixture (50 to 200 units/ml and 0.6 to 2.4 units/ml, respectively). The digested tissue was dissociated further by syringe passage and the resulting cell

suspension was filtered (40 μm filter), washed with balanced salt solution *via* centrifugation, and plated in non-selective maintenance (NSM) medium containing phenol red-free, HEPES-buffered DMEM/F12, supplemented with 10% FBS, GlutaMAX™ (L-alanyl-L-glutamine; Invitrogen, Grand Island, NY, USA), 2-mercaptoethanol (Invitrogen), non-essential amino acids (Invitrogen) and antibiotic-antimycotic solution (Invitrogen). Viability of disaggregated cells from cryopreserved lung tissue was measured using a hemocytometer on an inverted light microscope and Trypan blue exclusion. All thawed cells were cultured for two passages in NSM medium prior to plating and expansion in selective media. Primary vascular endothelial (VE)-like cells were expanded on tissue culture-treated plastic coated with 0.1% gelatin in EGM-2 medium (CC-3162; Lonza, Walkersville, MD, USA) and pneumocytes/alveolar type II (ATII) cells were expanded on tissue culture-treated plastic coated with 0.1% gelatin in either HITES medium [RPMI 1640 medium supplemented with antibiotics, hydrocortisone (10 nM), insulin (5 μg/ml), transferrin (100 μg/ml), 17β-estradiol (10 nM), and sodium selenite (30 nM), supplemented with 5% FBS] or small airway epithelial cell medium (SAEC; Lonza) at 37˚C in 5% CO_2, 21% O_2. Fibroblast cells were expanded in NSM or DMEM. Potential stem cells were grown in mTeSR1 medium (Stem Cell Technologies, Vancouver, Canada).

Reverse transcription polymerase chain reaction (RT-PCR). To identify the expression of cell-specific marker genes in primary cell cultures derived from cryproserved lung tissue, RNA was extracted using an RNeasy Mini Kit (QIAGEN Inc, Valencia, CA, USA), followed by DNaseI digestion. cDNA synthesis was performed using 1 μg total RNA, a mixture of random 9-mer and oligo-dT priming, and M-MuLV reverse transcriptase (reagents from New England Biolabs, Ipswich, MA, USA). qPCR was performed in triplicate using SYBR Green Supermix (BioRad, Hercules, CA, USA) and a Mastercycler RealPlex2 instrument (Eppendorf, Hamburg, Germany). For size verification, PCR amplicons were separated and visualized on 4-12% polyacrylamide-tris base, boric acid, EDTA PAGE-TBE gels (Invitrogen/Life Technologies, Carlsbad, CA). The primers used were: surfactant protein B (*SFTPB*) (F, 5'-GGACATCGTCCACATCCTTA ACAAGATG-3'; R, 5'-ATTGCTGCTCGGAGAGATCCTGTGT GTG-3'); surfactant protein C (SFTPC) (F, 5'-CCTGGCACCTGC TGCTACATCATG-3'; R, 5'-TAGTAGAGCGGCACCTCGCCACAC-3'); collagen (*COL1A1*) (F, 5'-ACATCCCACCAATCACCTGCG TAC-3'; R, GTCTCCCTTGGGT CCCTCGACGC-3'); aquaporin-5 (*AQP5*) (F, 5'-GTCAACGCGCT CAACAACAACACAAC-3'; R, 5'-AGCAGCCAGTGAAGTAGATT CCGAC-3'); ADP-ribosylation factor 1 (*ARF1*) (F, 5'-GCCAGTGT CCTTCCACCTGTC-3'; R, 5'- GCCTCGTTCACACGCTCTCTG-3'); Nanog homeobox (*NANOG*) (F, 5'-AGGACAGCCCTGATTCTT CCACCAG-3'; R, 5'-AGTTC TTGCATCTGCTGGAGGCTGAG-3'); and two pairs of primers to amplify all transcript variations of octamer-binding transcription factor 4 (*OCT4*) (OCT4-1: F, 5'-AGGCC GATGTGGGGCTCAC-3'; R, 5'-AGCTTCCTCCACCCACTTCTGC-3' and OCT4-2: F, 5'-ATGG CGGGACACCTGGCTTC-3'; R, 5'-AGGTCCGAGGATCAACCC AGC-3').

Two-dimensional differential gel electrophoresis (DIGE). For DIGE experiments, protein was prepared from fresh and thawed tissue portions and protein expression profiles were acquired, as previously described (8). Briefly, an internal control sample (Cy2 CyDye; GE LifeSciences, Pittsburgh, PA, USA) was prepared by mixing duplicate volumes of fresh/thawed samples, while the remainder of each sample was labeled with either Cy5 or Cy3 fluorescent CyDyes (GE LifeSciences) using a dye-swapping protocol. Two samples (Cy3 and Cy5) and the internal control sample mix are combined and adsorbed onto an immobilized pH gradient (IPG) DryStrip gel for a 12-h period. The IPG strips are then placed on an isoelectric focusing unit for focusing proteins based on pI. Samples were run in triplicate on two different pH gradients (4-7, 6-11) for isoelectric focusing. For second-dimension molecular weight separation, horizontal sodium dodecyl sulphate polyacrylamide gel electrophoresis (SDS-PAGE) was performed using plastic-backed gels on an HPE FlatTop Tower (The Gel Company, San Francisco, CA, USA). Gels were then scanned using a Typhoon TRIO™ Plus scanner (GE LifeSciences) for detection of fluorescence and quantified using Progenesis SameSpots Image Analysis software (Nonlinear Dynamics, Durham, NC, USA) with statistical analysis capabilities. Spot picking for protein ID *via* mass spectrometry was performed on an Ettan Spot picking robot (GE LifeSciences). Each sample was run in triplicate. For in-sample variation experiments, three tissue sections per patient sample were processed independently.

Matrix-assisted laser desorption/ionization-mass spectrometry imaging (MALDI-MSI) molecular mapping. As a high-end complementary approach, fresh dissected lung cubes, PDX-CP thawed lung cubes and primary cells cultured from dissociated fresh-thawed tissue were analyzed by MALDI-MSI for comparison of molecular 'maps' for cryopreserved tissues or cells. Lung tissue cubes were imbedded in optimal cutting temperature (OCT) compound for proteomic and glycomic analyses, or in poly(*N*-(2-hydroxypropyl)methacrylamide) for lipidomic analyses (19). Primary cells were plated directly on Bruker ITO (indium-tin oxide-coated) conductive slides and cultured before processing and analyses. For OCT-embedded tissue and native protein/peptide analysis, 10-12 μm sections were mounted on Bruker ITO conductive slides, and, as with cells, processed for protein analysis with a series of ethanol washes and placed in a vacuum dessicator for 5 min prior to matrix application. Tissue slices were coated with α-cyano-4-hydroxycinnamic acid (CHCA) matrix at 60 mg/ml in 75% acetonitrile and 0.1% TFA using an Image Prep (Bruker Daltronics, Fremont, CA, USA). This same ImagePrep sprayer was used to spray a fine-layer of trypsin to generate peptide profiles, or protein *N*-glycanase F for *N*-linked glycans. After enzyme spraying, tissue slides were incubated for 2 h at 37˚C in a humidified chamber, followed by matrix application [CHCA for peptides; 2,5-dihydroxybenzoic acid (DHB) for glycans]. For lipidomic analyses, no tissue processing was performed, as DHB matrix was directly applied to the 10-12 μm tissue slices cut from tissue embedded in poly(*N*-(2-hydroxypropyl)methacrylamide) and directly analyzed. Post matrix application and prior to MS analysis, slides were placed in the dessicator for 15 min. Digital images of the prepared sections/cells were acquired using a high resolution flatbed scanner (Hewlett-Packard, Palo Alto, CA, USA). Mass spectra were acquired using an AutoFlex III (Bruker Daltonics) instrument operating at 200 Hz in the linear mode over a mass range of 2,000-20,000 m/z for proteins and peptides, and a Bruker Solarix 70 Fourier transform ion cyclotron resonance (FTICR) mass spectrometer was used for imaging of the lipids and N-glycans. Mass spectra were accumulated using 200 laser shots from each spot on the tissue. Images of differentially expressed glycans were generated to view the expression pattern of each analyte of interest using FlexAnalysis 3.2 software (Bruker Daltonics). The intensity of each signal over the entire mass range acquired was plotted as a function of location on the tissue, allowing the visualization of the location of each m/z detected. Peak picking and three-way statistical comparisons were generated using v. 2.2 of ClinProTools (Bruker Daltonics).

Flow cytometric analysis of mitochondrial membrane potential. This was measured by MitoTracker Green FM (Life Technologies, Grand Island, NY, USA) and confirmed using 3,3'-dihexyloxacarbocyanine iodide ($DiOC_6$; final concentration 100 nM, λ_{ex} 488nm, λ_{em} 529 nm). Adherent and floating cells were harvested, washed once in PBS, and incubated with $DiOC_6$ for 20 min at 37˚C. Following incubation, cells were washed with ice-cold PBS, re-suspended in 0.5 ml of PBS on ice, and immediately analyzed (cells showing decreased $DiOC_6$ fluorescence represents cells with decreased mitochondrial membrane potential).

Statistical analyses. When possible, a minimum of three patient-specific samples corresponding to similarly diagnosed lung cancer and tissue pathologies were processed and compared (Hollings Cancer Center and SCTR/CTSA Biostatistics Cores, Drs. Liz Garrett-Mayer and Dr. Paul Nietert). All sample preparations and analyses were run in triplicate (on separate occasions) to account for cube-to-cube variations. Results are expressed as means with standard deviations (SD). Unless otherwise indicated, $p<0.05$ is deemed significant.

Results

Architectural impact of expansion-perfusion rate/volume and cryoprotectant solution formulations. Histological sections were examined by our pulmonary pathology specialist (Dr. Ellen Riemer) to document pathologies and artifacts. Brown-Brenn gram stain was included to assess gram-positive/negative bacterial infection. Infiltrating lymphocytes, anthracotic pigment and hemosiderin-positive macrophages were commonly detected (data not shown) in both PDX-CP and standardly (sCP)-prepared tissues. Rather than using limiting human tissue, an acute ischemia/reperfusion pig model was used initially to establish rate/volume limits for PDX-perfusion conditions (Figure 1). A wide range of expansion volumes (0.6 to 1.8 × tissue volume) was tolerated at rates up to 4 cc/min without architectural damage (Figure 1C and D). Greater than two-fold volumes of expansion resulted in primarily lymphatic expansion (Figure 1A). Rates of expansion faster than 4 cc/min commonly led to lymphatic expansion or tearing (Figure 1B) which was exacerbated post-thawing (data not shown). Lung pathologies that alter tissue compliance (*e.g.* less compliant fibrotic tissue) and changes in sCP viscosity are anticipated to impact these limits.

Cryoprotectant formulations were then compared to assess structural damage caused by crystal formation during controlled-rate freezing to −80˚C. A variety of non-toxic cryoprotectant formulations containing trehalose, phospholipids, surfactants, perfluorocarbons, protease inhibitors and other components were compared to and improve upon the standard cryoprotectant solution (sCP; 10% DMSO, 20% FBS in DMEM/F12). Increased formulation viscosities impacted expansion rate over volume (not shown). Cryosubstitution (aqueous replacement with methanol below −80˚C) was performed prior to processing for H&E staining to fix and observe crystals formed in tissue during the freezing process. Crystal imprints were accentuated at −80˚C compared to −90˚C, albeit with some distortion (2, 14, 16). As shown, much greater crystal formation and pleural distortion-contraction were observed using sCP rather than modified (PDX-CP) formulations (Figure 2).

Architectural integrity results obtained with pig lungs were verified with human lung tissue samples (Figure 3). Fresh lung lobectomy samples from patients with COPD/lung cancer were either directly-fixed by immersion in 4% paraformaldehyde (PFA; Figure 3, panels A-C), expansion-perfused with PDX-CP before fixation with PFA (Figure 3D-F), or expansion-perfused, cryopreserved for one week at −80˚C, thawed and immersion-fixed with PFA (Figure 3G-I). Low and high magnification images demonstrate preservation of tissue/cellular architecture in alveolar and bronchiolar regions. While minimal changes were detected, we did observe some damage to cilia in the ciliated epithelium of the upper airways in thawed tissues (cf. arrow regions in Figure 3 panels C, F and I). However, we did observe recovery of cilia after short-term *in vitro* culture (data not shown). The advantage this method affords is that this tissue was not inflation-fixed with formalin, thus preserving the ability to measure proteins, lipids and nucleic acids or harvest viable cells without sacrificing the ability to view lung architecture and histology at a later time.

RNA integrity assessments. RINs were compared in several samples from patients with COPD/lung cancer lung lobectomy that were either expansion-perfused with PDX-CP before RNA extraction or expansion-perfused, cryopreserved for a week at −80˚C and thawed before RNA extraction. No difference in RIN values was observed between pre- and post-cryopreservation samples (pre-cryo $RIN_{(avg)}$=7.92; SD=0.89, post-cryo $RIN_{(avg)}$=8.17; SD=1.00, N=8). Fresh and PDX-CP cryopreserved-thawed lung cubes were also compared for protein integrity (Figure 4), showing only minor changes, suggesting minimal degradation or protein modifications as a consequence of cryopreservation and thawing. We have repeated this analysis on samples stored at −80˚C for as long as three months with similar results (data not shown).

Cell viability in PDX-CP lung tissue. A comparison of two different dissociated samples after 24 h in suspension culture demonstrated a range of 81-53% viability in thawed compared to fresh tissues, with the high-viability tissue having a lower percentage of dead cells (Figure 5). The range in cell viabilities may indicate differences in extracellular matrix (ECM) components, such as those contributing to fibrosis. Explant lung tissue from a patient with IPF was similarly studied for cell viability and growth (Figure 6). One cryovial containing three 125 mm^3 cubes was thawed and processed for i) PFA fixation and H&E staining (Figure 6A), ii) placed directly in a gelatin-coated dish for organ outgrowth culture (Figure 6B) or iii) enzymatically-dissociated, plated in culture (Figure 6C-E) and passaged (Figure 6F and G). A more varied population of

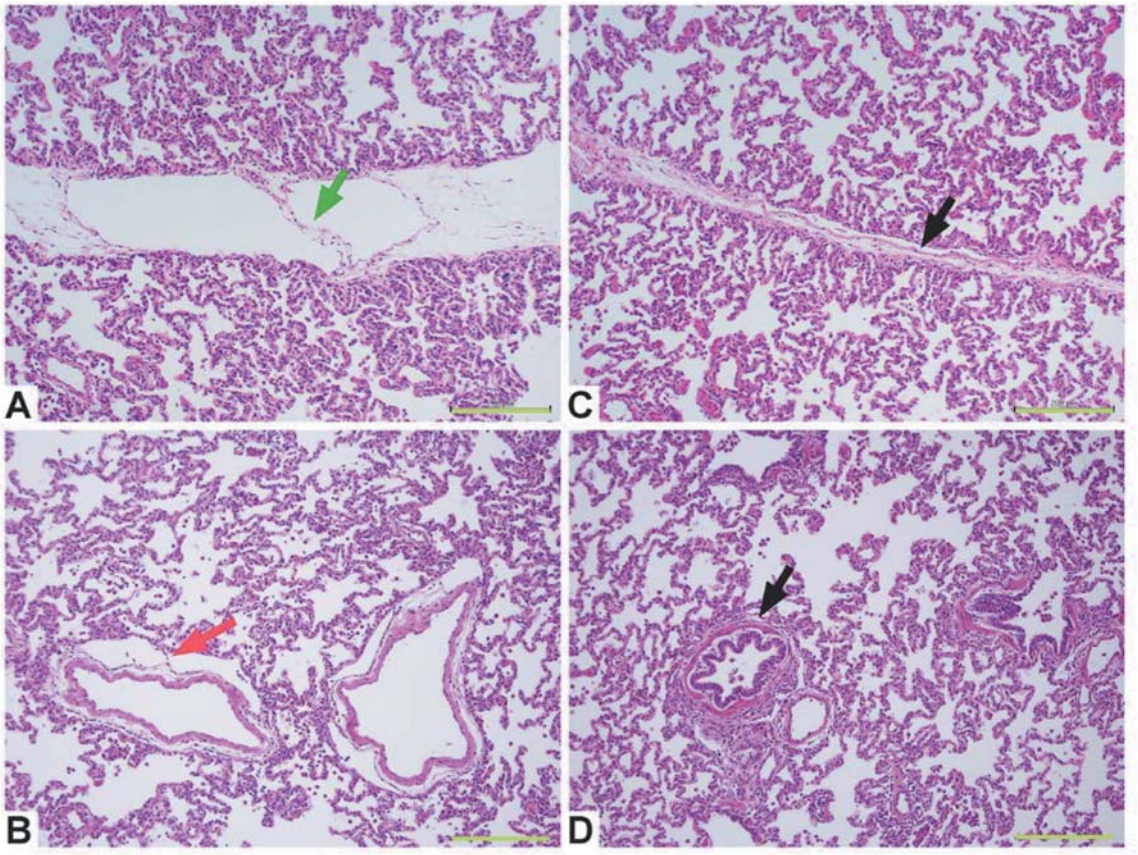

Figure 1. *Artifacts incurred by large volumes and high rates of expansion perfusion. Freshly-explanted pig lungs were expansion-perfused in standard cryoprotectant (10% dimethyl sulfoxide, 20% fetal bovine serum in DMEM/F12), fixed in 4% PFA and processed for H&E staining. Overexpansion (2× v/v, 4 cc/min; panel A) and higher rates of expansion (6 cc/min; panel B) caused mostly lymphatic expansion/tearing (green/red arrows). Panels C and D show two examples of normal lymphatics (black arrows) at 1.8× and 0.6× expansion and 4 cc/min rate. (Scale bars: green, 200 μm).*

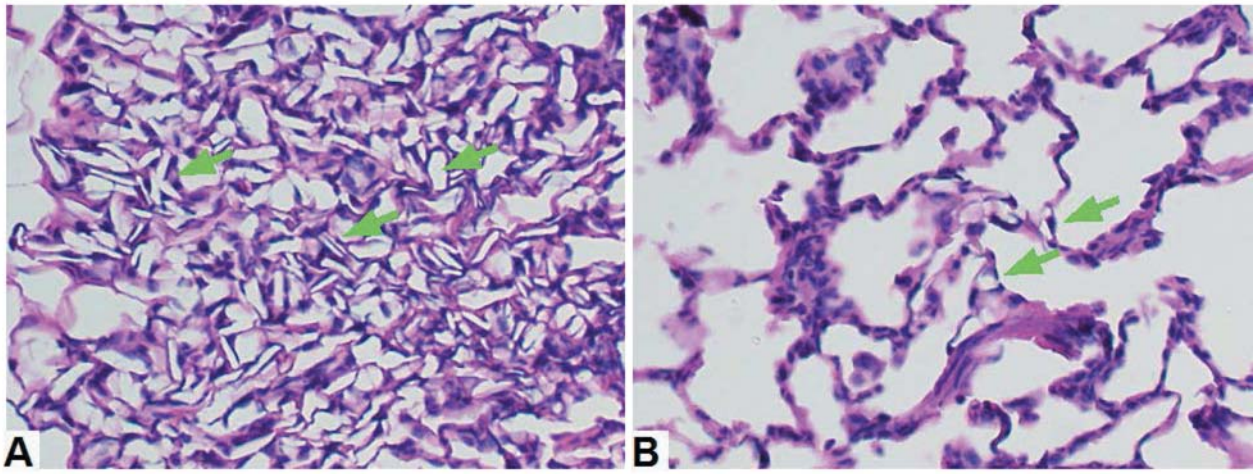

Figure 2. *Cryosubstitution to detect crystals and extracellular matrix distortion. Freshly-explanted pig lungs were expansion-perfused in standard (left) and pseudo-diaphragmatic expansion-cryoprotectant perfusion (PDX-CP) (right) cryoprotectant solution, frozen to −80˚C at 1˚C/min and subjected to substitution of aqueous with methanol, prior to processing for H&E staining. Much greater crystal formation and tissue distortion (contraction) were observed in standard cryoprotectant (panel A) than in PDX-CP (panel B). Green arrows show examples of crystal formation.*

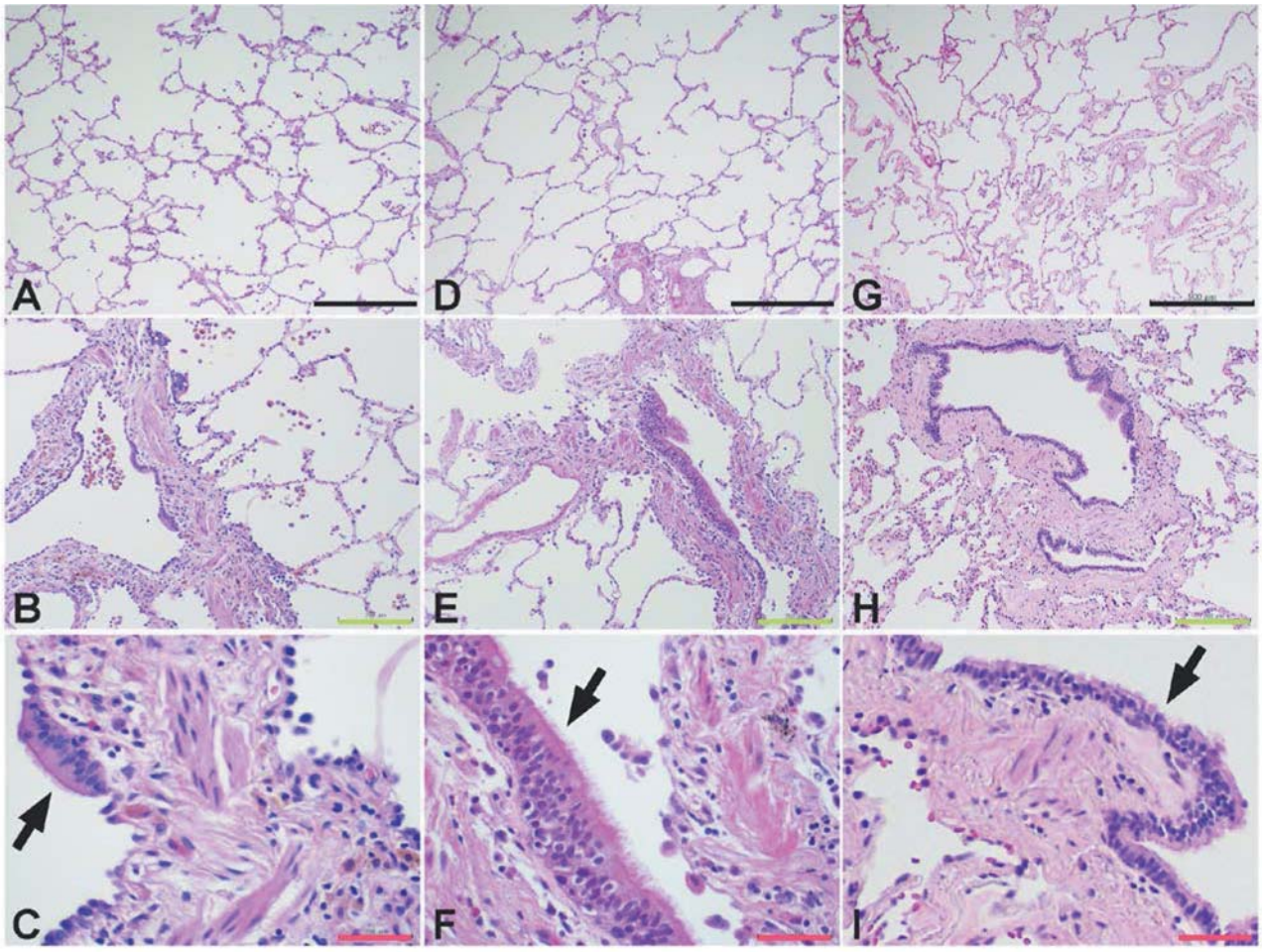

Figure 3. *Lung tissue architecture maintained after thawing. Human lobectomy tissue cubes (IRB designation BAAT001 and SPYR008) were directly fixed in 4% paraformaldehyde at 4˚C (A-C), fixed after expansion/perfusion with pseudo-diaphragmatic expansion-cryoprotectant perfusion (PDX-CP; 1× v/v, 4 cc/min; D-F) or fixed after cryopreservation, storage for a week at −80˚C and thawing (G-I) and processed for hematoxylin and eosin staining of 6 μm sections. No loss of tissue/cellular architecture was observed in bronchoalveolar regions. Of note, some damage to ciliated epithelium in the upper airways of thawed tissues was observed (compare arrow regions in I to C, F). (Scale bars: black, 500 μm; green, 200 μm; red, 50 μm).*

cells was obtained *via* enzymatic digestion, including upper airway ciliated epithelium, fibroblasts, vascular endothelial cells and lower airway ATI and ATII cells. Outgrowth fibroblasts (Figure 6B) were assessed for collagen and activation marker expression, demonstrating a typical fibrotic lung fibroblast phenotype (data not shown). Cell viability 24 h after enzymatic digestion was about 40%, supporting the notion that more advanced fibrosis negatively impacts dissociation of viable cells. In fact, tissue examination (Figure 6A and data not shown) revealed multiple signs of mixed acute and chronic inflammation, including extensive immune cell infiltrates, smooth muscle/fibroblast hyperplasia, squamous metaplasia, thickened secretions and inflammatory cells in airways. Nevertheless, surviving primary cell types were estimated to collectively maintain a fair doubling time of 31 h. Specialized cell types were identified by RT-PCR of cell-specific gene expression in primary cell cultures derived from cryopreserved tissue (Figure 6H). Thawed lung samples were enzymatically-dissociated before culturing. Type II pneumocytes were identified by their expression of SPC and SPB, type I pneumocytes by their expression of AQP5 and fibroblasts by their expression of COL1A1. Potential stem cells also survived many days post-thawing and could be identified by expression of Nanog and OCT4 (Figure 6I). This does not constitute an exhaustive list of viable cell types that could be retrieved. However, it does illustrate that various populations can be retrieved from cryopreserved lung tissues of various pathologies, including IPF. Such primary cells could be used to reconstitute hollow fibers in a "Bottom-Up' scenario, as we described previously (4) and used to facilitate differentiation of

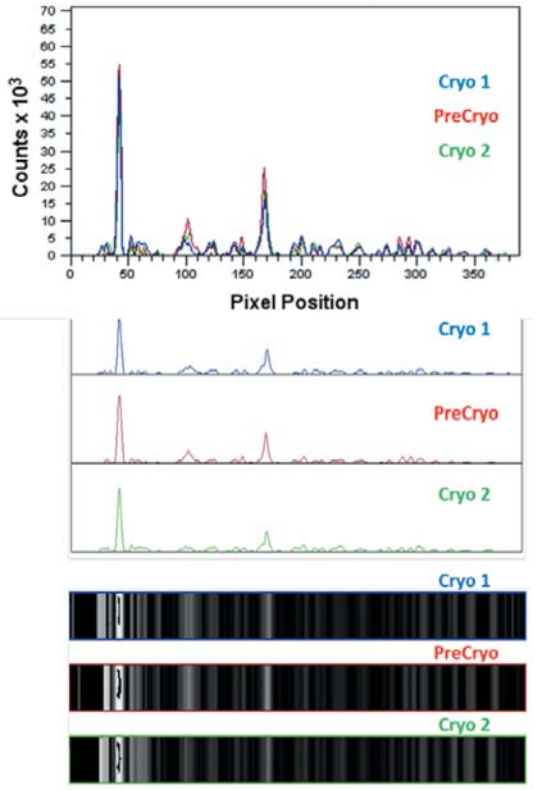

Figure 4. *Protein integrity maintained in thawed lung tissue. 'Fresh' patient lobectomy tissue cubes, prior to preservation ("PreCryo") and post-thaw ("Cryo1" and "Cryo2") were homogenized at 4˚C in isotonic phosphate buffered saline containing protease inhibitors, solubilized in 4× Laemli sodium docecyl sulfate-polyacrylamide gel electrophoresis buffer and 5 μg total protein per sample run on a 4-12% Bis-Tris gel at 200 V using 3-(N-morpholino)propanesulfonic acid MOPS buffer (bottom). Analysis of the protein profiles (middle, individually; top, overlay) showed only minor changes in protein profiles suggesting minimal degradation or protein modifications as a consequence of preservation and thawing.*

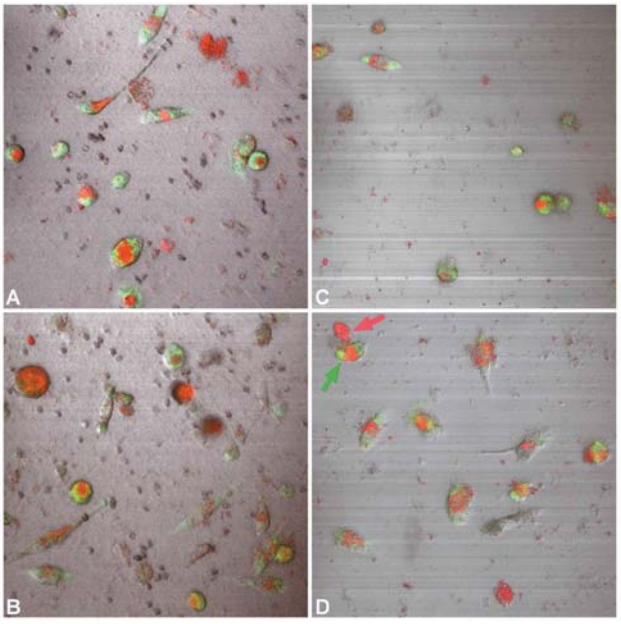

Figure 5. *Cell viability in fresh vs. thawed lung tissue. Human lung lobectomies (BAAT004, A and C; SPYR008, B and D) were enzymatically digested for cell isolation from fresh samples (A and B) or thawed after 14 days stored at –80˚C samples (C and D). Cells from digested cubes were plated in suspension for 24 h prior to MitoTracker (Green) FM labeling of viable cells and nuclear counterstain (red). For BAAT004, we observed 81% viability and for SPYR008, 53% viability in thawed vs. fresh samples, with a greater fraction of dead cells in the latter (which may reflect more fibrotic tissue).*

specialized cell phenotypes [*e.g.* SPB-positive; ref. (9)]. 'Bottom-Up' approaches include those that utilize simple combinations of components, such as specific primary cell types and ECM molecules.

Protein post-translational product and overall molecular integrity of tissues. In addition to standard RNA integrity and cell viability assessments, DIGE and MALDI-MSI molecular mapping were also used, as high-end approaches, for analysis of fresh and thawed tissues to determine overall quantitative and spatial molecular integrity, respectively. DIGE serves as a highly visual, but non-spatial indicator of 'before and after' differences. DIGE is exceptionally powerful for detection of changes in relative abundance of post-translationally modified forms of any given protein (*e.g.* changes in multiply phosphorylated proteins). As exemplified in Figure 7, such changes are easily visualized by changes in peak volumes of the isoforms for given proteins on a computer-generated topographical display. Table II shows that minimal differences in proteomic profiles were detected between patient-derived lung tissues pre- and post-cryopreservation. A much larger number of statistically significant spots, with larger fold changes, were observed when comparing lung tissue samples from patients with COPD *versus* those with IPF, as compared to pre- or post-cryo tissues from the same patient or disease type. By far, the most significant changes between pre- *versus* post-cryopreservation samples (and among post-cryo replicates) were proteins that were washed-out during the perfusion process (*e.g.* erythrocyte and serum proteins).

MALDI-MSI molecular mapping served as a high-end complementary approach for complete molecular profiling. Fresh-dissected lung cubes, cryopreserved-thawed lung cubes and primary cells cultured from dissociated fresh/thawed tissue were analyzed by this method. As shown in Figure 8, *N*-linked glycan expression in lung tissue showed minimal spatial differences when comparing 'before and after' tissues.

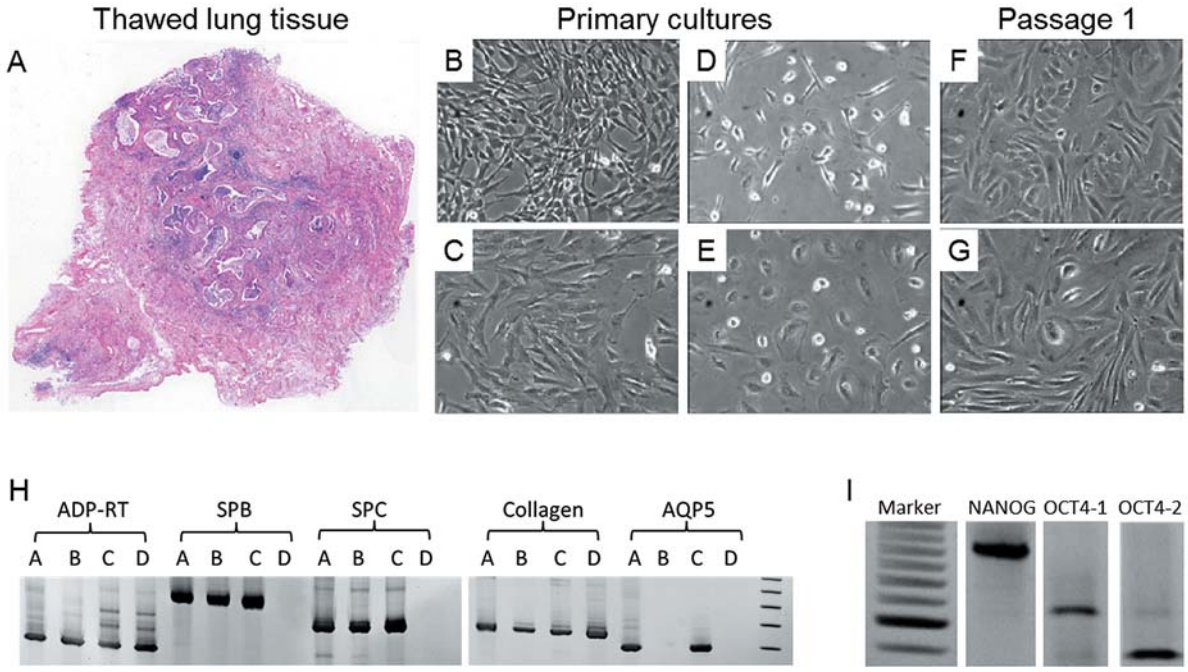

Figure 6. *Viability of cryopreserved lung cells from a patient with idiopathic pulmonary fibrosis. Explanted lungs from a transplant patient with lung fibrosis were cryopreserved using pseudo-diaphragmatic expansion-cryoprotectant perfusion (PDX-CP). One cryovial containing three 125 mm3 cubes was thawed after 14 days in storage at −80˚C and processed with 4% neutral buffered paraformaldehyde (PFA) fixation and H&E staining (A), or placed directly in a gelatin-coated dish for outgrowth culture (B), or enzymatically dissociated, plated in culture (C-E) and passaged (F, G) to expand multiple cell types. Panel H: Primary cells derived from PDX-CP cryopreserved tissue express cell-specific genes in culture. Reverse transcription polymerase chain reaction RT-PCR products separated by polyacrylamide gel electrophoresisPAGE. Samples were taken from a IPF patient explant during transplant surgery and cryopreserved; then later, thawed and enzymatically-dissociated before culturing. RNA was extracted from four samples for analyses: A: whole lung tissue (RNA extracted before cryopreservation); B, alveolar epithelial cell culture (SAEC medium, 1-week post-thawing/dissocation); C: alveolar cell culture (2-week post-thawing/dissociation); ADP-RT: housekeeping gene/normalization control (ARF1); SPB: surfactant protein B, type II pneumocyte marker (and possibly, bronchiolar Clara cells); SPC: surfactant protein C, type II pneumocyte marker; collagen: fibroblast marker (COL1A1); AQP5: aquaporin 5, type I pneumocyte marker. Last lane is a molecular weight marker. Panel I: Stem cells can be cultured from PDX-CP cryopreserved lung tissue. Enzymatically-dissociated cells (same IDF patient as Panel H) were cultured for seven days in mTeSR1 medium and RNA subsequently analyzed for expression of stem cell cell markers octamer-binding transcription factor 4 (OCT4) (2 separate primer sets used to amplify all transcript variants) or Nanog homeobox (NANOG)by RT-PCR. Prominent band in 25-bp marker (lane 1) is 125 bp.*

Table II. *Quantitative, 2-D differential gel electrophoresis (DIGE) of total protein demonstrates minimal differences between pre-/post-cryopreserved PDX-CP lung tissues. The number of spots that demonstrated increased (bold) or decreased (underlined) levels of protein quantify differences are shown. DIGE was performed by labeling protein samples with either Cy3 or Cy5 minimal fluorescent dyes (plus internal control Cy2), combining the samples, and separating protein spots by isoelectric focusing (1st dimension) and SDS-PAGE (2nd dimension). Each sample was run in triplicate. For in-sample variation experiments, three tissue sections per patient sample were processed independently.*

Comparison	Total no. of spots	Total no. of different spots (p<0.05)	Largest fold change (p<0.05)	No. of spots with fold change >2.0 (p<0.05)	No. of spots with fold change >3.0 (p<0.05)
Pre *vs*. Post Cryo (COPD)	2210	29	6.3	13/2	0/1
Pre *vs*. Post Cryo (IPF)	1521	63	7.9	14/7	7/6
COPD *vs*. IPF (post-cryo)	1587	249	12	59/56	16/29
In-sample variation (post-cryo COPD replicates)	2951	41	2.5	6	0

Pre-cryo, samples processed immediately after pseudo-diaphragmatic expansion cryoprotectant-perfusion (PDX-CP) and without cryopreservation at –80˚C; Post-cryo, samples processed after thawing PDX-CP-prepared and cryopreserved samples after storage for 14 days; COPD, chronic obstructive pulmonary disease; IPF, idiopathic pulmonary fibrosis.

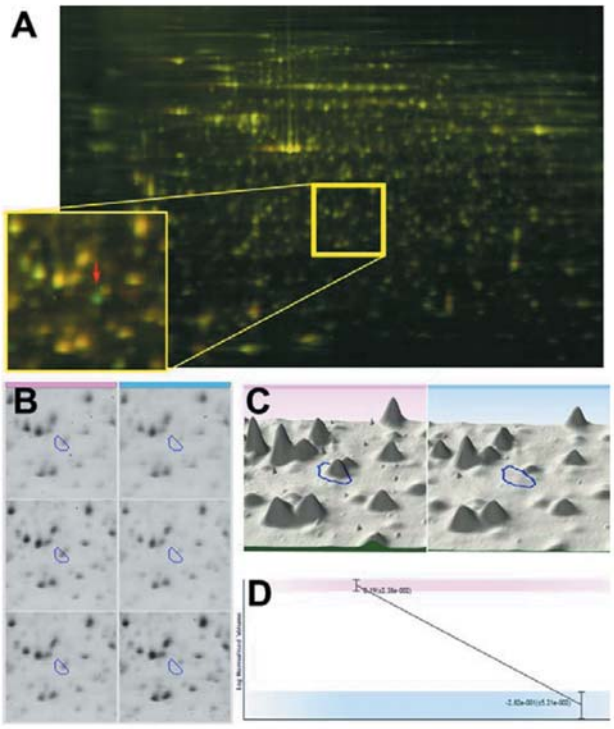

Figure 7. *Utility of differential gel electrophoresis (DIGE) to detect unique and minute differences in protein expression in lung cells as a function of specimen source or environment. A: Two-color image of 24 cm DIGE gel of porcine (Cy3-labeled, green) and pygmy sperm whale (Cy5, red) lung cells using pH 4-7 IPG strips. Expanded box indicates region of high protein profile similarity, and with a major significant difference in expression of one protein (red arrow). B and C: The expanded regions of porcine (below magenta bar) and pygmy sperm whale (below cyan bar) samples run in triplicate (3 DIGE gels) Protein spot represented in expanded box in A with significantly differing expression levels (D) between species is bordered with blue line.*

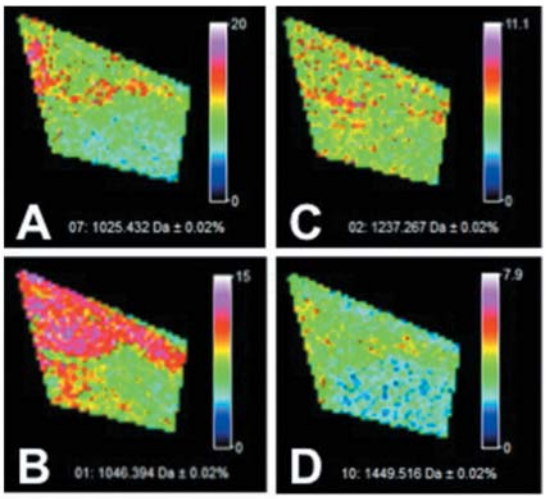

Figure 8. *N-Linked glycan expression in lung tissue as determined by matrix-assisted laser desorption mass spectrometric imaging. Lung tissue embedded in optimized cutting temperature compound was frozen-sectioned (10 μm) and mounted on ITO conductive slides, and processed with a series of ethanol washes. Processed slides were sprayed with protein N-glycanase F, incubated for 2 h at 37˚C in a humidified chamber, followed by matrix application (2,5-dihydroxybenzoic acid (DHB) 30 mg/ml). Tissues were imaged using a Bruker Autoflex III mass spectrometer in reflection mode, and analyzed in FlexImaging (Bruker Daltonics). m/z Peak profiles for one tissue are shown (A: 1025.432 Da; B: 1046.394 Da; C: 1237.267 Da; D: 1449.516 Da).*

To demonstrate proof-of-concept that cryopreserved lung tissue can be used for advanced mechanistic and therapeutic studies in a 'Top-Down' scenario (to complement the 'Bottom-Up' approach shown in Figure 6), we tested *ex vivo* the impact of patient-specific lung tissue on growth and function of perfused cells, in this case, H358 non-small cell lung adenocarcinoma [$p53^{-}$, wild-type epidermal growth factor receptor ($EGFR^{wt}$), wild-type serine/threonine kinase 11 ($LKB1^{wt}$); ref. (3, 18, 22, 24, 25)]. H358 cells grown in monolayer culture had strikingly different morphology from those perfused into patient lung tissue (epithelial-to-mesenchymal transition, under investigation), even after only 5 h of co-culture (Figure 9). Differences in H358 cell growth were observed between thawed patient tissues after six days of co-culture (Figure 9E and F) even though cell viability was similar (MitoTracker Green FM; data not shown). Conventional H&E and immunostains were augmented by MALDI-MSI imaging of proteins from tissue alone, tissue-plus-cells and cells-alone (Figure 9G-J). We were able to correlate morphology to specific m/z protein signatures ('heat map' images) even though quite a few total differences were detected (Figure 9J). It is likely that the uniquely expressed species originate from either the tissue or cell in response to discrete cell–cell and cell–matrix interactions, thus contributing to lung cancer patient-specific molecular profiles (23). These results demonstrate that such an approach, enabled by the PDX-CP protocol, may prove advantageous for identifying specific protein (and lipid) targets in high-throughput mechanistic and therapeutic studies, and feedback to stratify patients based on profiling of small biopsies.

Discussion

A majority of studies reported to date have attempted to determine mechanisms or biomarkers of lung disease using a very low number of lung tissue samples in control and cancer/disease arms (often less than n=6 total), thereby significantly limiting the impact of the studies. Fresh human samples are difficult to obtain and thus, when available, must be utilized in as many different studies and molecular

approaches as possible. However, the number of fresh tissues obtained from control and diseased specimens can severely affect the time required to obtain appropriately powered data, often requiring years before sufficient sample size is obtained.

An alternative to using fresh tissue is the utilization of specimens from biorepositories, where a larger number of disease-specific and control tissues can be obtained at one time. One shortcoming of this path is that the various preservation protocols currently used prior to storage limit their utility in the analytical approaches for mechanistic or biomarker investigations (see Table I). For example, traditional formalin fixation is incompatible with protein/nucleic acid analysis; use of RNAlater can limit protein and metabolomic assessments; and snap-freezing in liquid nitrogen does not provide lung architecture that is adequate for histological description, cell identification with immunohistochemistry or cell viability. Very few tissue preservation techniques allow for recovery of viable cells that can be cultured or used for experiments. Conversely, our PDX-CP method allows the tissue from human or animal subjects to be used for all of these types of analyses (Table I). Thus, the nature of these studies can be more versatile, improving biomarker detection in standard/conventional –omic and immuno-histochemical studies and facilitating development and implementation of high-throughput drug discovery platforms. In addition, the PDX-CP approach offers the added advantage of long-term 'batching' of disease-specific or control tissue samples, permitting a higher number of replicates to be examined at one time, while still allowing for all analytes to be measured as in fresh tissue. Intact lung tissues and an array of primary cells and matrix components thereby derived will be materials for such high-end personalized medicine studies.

Current pulmonary care and treatment are in dire need of accurate models for mechanistic and therapeutic advancements related to lung injury and disease. Lung biospecimens most often fail to provide a sufficient variety of high quality analytes to make such lung samples useful for these pulmonary studies (5, 11-13, 15, 20). Arguably, tissue samples are more representative of diseased microenvironments than assembled three-dimensional (3D) cell/matrix co-culture systems. However, 3D systems are very useful for delineating key disease elements for focused therapies. The PDX-CP approach provides both complex tissue samples and a source for extractable components. Thawed pieces of lung tissue are amenable to all post-acquisition processing methods applied to fresh tissue. Primary cell types and matrices have been isolated and expanded *in vitro* and whole pieces cultured *ex vivo* for several days after thawing (Figures 6 and 9). As illustrated in Table I, the PDX-CP lung tissue technology offers a simple solution to overcome problems associated with banking of lung tissue samples for specialized uses by a wide variety of methods. We believe that universal implementation of the PDX-CP protocol would greatly benefit and increase acquisition of samples from biorepositories by researchers around the world, due to inherent analytical flexibility of samples preserved *via* PDX-CP.

Acknowledgements

The Authors would like to thank Dr. Rita M. Ryan for critical review of and insightful comments on this manuscript. This work was supported in part by grants from the National Institutes of Health (HL085738, JEB) and the BP/The Gulf of Mexico Research Initiative (DDS). The Gulf of Mexico Research Initiative is a 10-year independent research program, established through a $500 million financial commitment from BP to investigate effects of the Deepwater Horizon incident.

References

1 Annual smoking-attributable mortality, years of potential life lost, and economic costs – United States, 1995-1999. MMWR Morbidity and mortality weekly report *51*: 300-303, 2002.
2 Brockbank KG, Chen ZZ and Song YC: Vitrification of porcine articular cartilage. Cryobiology *60*: 217-221, 2010.
3 Georges RN, Mukhopadhyay T, Zhang Y, Yen N and Roth JA: Prevention of orthotopic human lung cancer growth by intratracheal instillation of a retroviral antisense K-ras construct. Cancer Res *53*: 1743-1746, 1993.
4 Grek CL, Newton DA, Qiu Y, Wen X, Spyropoulos DD and Baatz JE: Characterization of alveolar epithelial cells cultured in semipermeable hollow fibers. Exp Lung Res *35*: 155-174, 2009.
5 Hatzis C, Sun H, Yao H, Hubbard RE, Meric-Bernstam F, Babiera GV, Wu Y, Pusztai L and Symmans WF: Effects of tissue handling on RNA integrity and microarray measurements from resected breast cancers. J Natl Cancer Inst *103*: 1871-1883, 2011.
6 Jemal A, Siegel R, Ward E, Hao Y, Xu J, Murray T and Thun MJ: Cancer statistics, 2008. CA Cancer J Clin *58*: 71-96, 2008.
7 Kap M, Smedts F, Oosterhuis W, Winther R, Christensen N, Reischauer B, Viertler C, Groelz D, Becker KF, Zatloukal K, Langer R, Slotta-Huspenina J, Bodo K, de Jong B, Oelmuller U and Riegman P: Histological assessment of PAXgene tissue fixation and stabilization reagents. PLoS One *6*: e27704, 2011.
8 Kondo T and Hirohashi S: Application of highly sensitive fluorescent dyes (CyDye DIGE Fluor saturation dyes) to laser microdissection and two-dimensional difference gel electrophoresis (2D-DIGE) for cancer proteomics. Nat Protoc *1*: 2940-2956, 2006.
9 Mancia A, Spyropoulos DD, McFee WE, Newton DA and Baatz JE: Cryopreservation and *in vitro* culture of primary cell types from lung tissue of a stranded pygmy sperm whale (Kogia breviceps). Comp Biochem Physiol C Toxicol Pharmacol 2011.
10 Minna JD, Roth JA and Gazdar AF: Focus on lung cancer. Cancer Cell *1*: 49-52, 2002.
11 Moore HM: The NCI Biospecimen Research Network. Biotech Histochem *87*: 18-23, 2012.
12 Moore HM, Kelly A, Jewell SD, McShane LM, Clark DP, Greenspan R, Hainaut P, Hayes DF, Kim P, Mansfield E, Potapova O, Riegman P, Rubinstein Y, Seijo E, Somiari S, Watson P, Weier HU, Zhu C and Vaught J: Biospecimen Reporting for Improved Study Quality. Biopreserv Biobank *9*: 57-70, 2011.

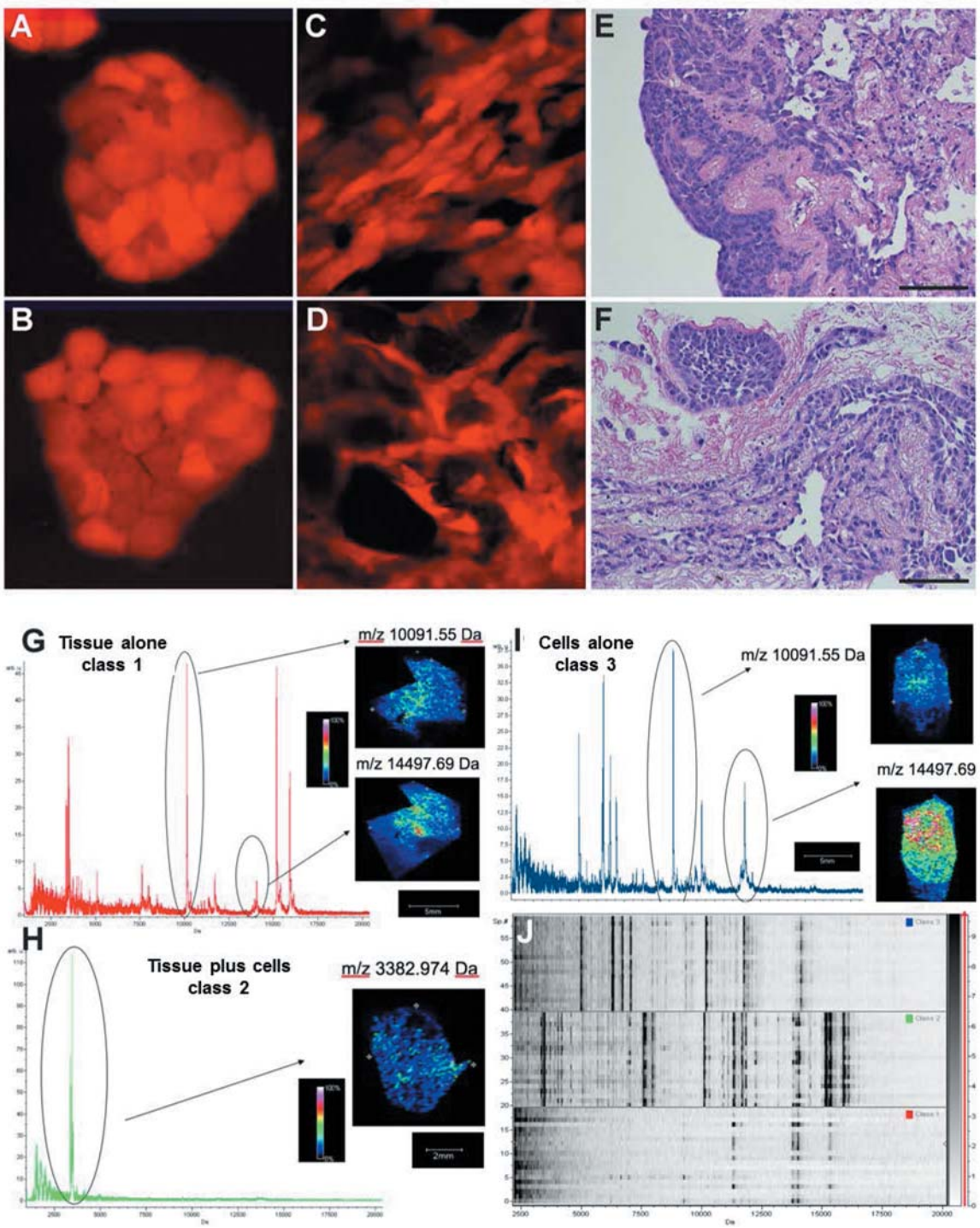

Figure 9. *Thawed lung tissue-cell co-cultures and matrix-assisted laser desorption mass spectrometric imaging (MALDI-MSI) molecular mapping. Red Fluorescent protein posiive (RFP+) H358 cells in monolayer culture (A and B) or perfused (5×105 cells) into SPYR002 (C and E) and SPYR003 (D and F) thawed lung cubes (~0.125 cm3). Expansion perfusion was repeated every 24 h with fresh media. Co-cultures at 72 h are shown (C and D; fluorescence, 50-μm wide images) and six days (E and F; H&E bright field, bar=100 μm). Cell shape and growth differ from monolayer to co-cultures and among tissues. MALDI-MSI of proteins was compared in lung tissue only (G, Class 1), tissue plus cells (H, Class 2) and cells alone (I, Class 3). Heat maps and particular m/z peak signatures could be correlated back to morphological features of serial H&E-stained sections. Multiple peak signatures differed significantly between classes corresponding to differing cell–cell and cell–matrix interactions. Biopsies may provide signatures useful for stratification.*

13 Rimm DL, Nielsen TO, Jewell SD, Rohrer DC, Broadwater G, Waldman F, Mitchell KA, Singh B, Tsongalis GJ, Frankel WL, Magliocco AM, Lara JF, Hsi ED, Bleiweiss IJ, Badve SS, Chen B, Ravdin PM, Schilsky RL, Thor A and Berry DA: Cancer and Leukemia Group B Pathology Committee guidelines for tissue microarray construction representing multicenter prospective clinical trial tissues. J Clin Oncol *29*: 2282-2290, 2011.

14 Schenke-Layland K, Xie J, Heydarkhan-Hagvall S, Hamm-Alvarez SF, Stock UA, Brockbank KG and MacLellan WR: Optimized preservation of extracellular matrix in cardiac tissues: implications for long-term graft durability. The Annals of thoracic surgery *83*: 1641-1650, 2007.

15 Shen J, Wang D, Gregory SR, Medico L, Hu Q, Yan L, Odunsi K, Lele SB, Ambrosone CB, Liu S and Zhao H: Evaluation of microRNA expression profiles and their associations with risk alleles in lymphoblastoid cell lines of familial ovarian cancer. Carcinogenesis *33*: 604-612, 2012.

16 Song YC, An YH, Kang QK, Li C, Boggs JM, Chen Z, Taylor MJ and Brockbank KG: Vitreous preservation of articular cartilage grafts. Journal of investigative surgery: the official journal of the Academy of Surgical Research *17*: 65-70, 2004.

17 Spruessel A, Steimann G, Jung M, Lee SA, Carr T, Fentz AK, Spangenberg J, Zornig C, Juhl HH and David KA: Tissue ischemia time affects gene and protein expression patterns within minutes following surgical tumor excision. Biotechniques *36*: 1030-1037, 2004.

18 Steiner P, Joynes C, Bassi R, Wang S, Tonra JR, Hadari YR and Hicklin DJ: Tumor growth inhibition with cetuximab and chemotherapy in non-small cell lung cancer xenografts expressing wild-type and mutated epidermal growth factor receptor. Clin Cancer Res *13*: 1540-1551, 2007.

19 Strohalm M, Strohalm J, Kaftan F, Krasny L, Volny M, Novak P, Ulbrich K and Havlicek V: Poly[N-(2-hydroxypropyl) methacrylamide]-based tissue-embedding medium compatible with MALDI mass spectrometry imaging experiments. Anal Chem *83*: 5458-5462, 2011.

20 Vaught JB, Henderson MK and Compton CC: Biospecimens and biorepositories: from afterthought to science. Cancer Epidemiol Biomarkers Prev *21*: 253-255, 2012.

21 Viertler C, Groelz D, Gundisch S, Kashofer K, Reischauer B, Riegman PH, Winther R, Wyrich R, Becker KF, Oelmuller U and Zatloukal K: A new technology for stabilization of biomolecules in tissues for combined histological and molecular analyses. The Journal of molecular diagnostics: JMD *14*: 458-466, 2012.

22 Yamamoto Y, Sakamoto M, Fujii G, Kanetaka K, Asaka M and Hirohashi S: Cloning and characterization of a novel gene, DRH1, down-regulated in advanced human hepatocellular carcinoma. Clin Cancer Res *7*: 297-303, 2001.

23 Yanagisawa K, Shyr Y, Xu BJ, Massion PP, Larsen PH, White BC, Roberts JR, Edgerton M, Gonzalez A, Nadaf S, Moore JH, Caprioli RM and Carbone DP: Proteomic patterns of tumour subsets in non-small-cell lung cancer. Lancet *362*: 433-439, 2003.

24 Zou Y, Fu H, Ghosh S, Farquhar D and Klostergaard J: Antitumor activity of hydrophilic Paclitaxel copolymer prodrug using locoregional delivery in human orthotopic non-small cell lung cancer xenograft models. Clin Cancer Res *10*: 7382-7391, 2004.

25 Zou Y, Zong G, Ling YH, Hao MM, Lozano G, Hong WK and Perez-Soler R: Effective treatment of early endobronchial cancer with regional administration of liposome-p53 complexes. J Natl Cancer Inst *90*: 1130-1137, 1998.

Received March 10, 2014
Revised March 18, 2014
Accepted March 20, 2014